



AB INITIO THEORETICAL STUDY OF THE $\text{HO} + \text{CO} \rightarrow \text{CO}_2 + \text{H}$ ENVIRONMENTAL CHEMICAL REACTION

LORENA GERLI-CANDIA^A, NAHARA ORTIZ-VERGARA^A,
GUILLERMO SALGADO-MOR'AN^B AND DANIEL GLOSSMAN-MITNIK^{C,*}

^a Facultad de Ciencias, Univ. Católica de la Santísima Concepción, Concepción, Chile

^b Facultad de Ciencias Exactas, Universidad Andrés Bello, Concepción, Chile

^c Laboratorio Virtual NANOCOSMOS - CIMAV, SC - Chihuahua, Mexico

ABSTRACT

Atmospheric temperature affects both the absorption spectrum and the concentration of atmospheric gases. Gases with larger abundances and stronger absorption band intensities in the infrared region have a greater influence on the greenhouse effect. The purpose of this work is to provide an ab initio theoretical conformational model of the reaction between the OH radical and CO, which is used to model common environmental reactions. The geometric optimization of the studied structures was performed using Hartree-Fock (HF) methodology, B3LYP (Becke, three-parameter, Lee-Yang-Par) and the Moller-Plesset perturbation theory to the 2nd order (MP2), using the 6-311++G** basis set and Gaussian 09W software for all calculations. Three stationary structures and six transition structures were found and were characterized by their normal modes of vibration. Using this methodology, we discovered two possible paths for the studied reaction, which were characterized by their potential energy hypersurface. These paths are the geometric isomers cis and trans HOCO radicals that yield a ΔH for the general reaction of -34.51 kcal/mol. According to the Hammond postulate, which relates the similarity in transition states with the reactants or products, the transition states participating in the studied reaction have a similar energetic character to the reactants, which is generally observed in exothermic reactions.

KEYWORDS: Chemistry, Theory, Environmental Reaction



DANIEL GLOSSMAN-MITNIK
Laboratorio Virtual NANOCOSMOS - CIMAV, SC - Chihuahua, Mexico

*Corresponding author

1. INTRODUCTION

The increased reliability of quantum chemistry, along with an increase in computing power and a greater understanding of the processes governing the dynamics of chemical reactions, has led to the acceptance of computational chemistry as a useful tool in atmospheric chemistry [1]. Computational chemistry, along with other applications developed over the past decades, has been successfully used to support experimental atmospheric chemistry [2]. This branch of science has been primarily applied in two defined directions. First, computational chemistry has been used in the creation of mathematical models to describe the relationship between primary pollutant emissions and resulting secondary pollutant concentrations. Secondary pollutants are produced by the chemical reactions that occur in the air during the transport and dispersion of the primary pollutants. Second, computational chemistry has been applied to study the reaction mechanisms, conformational energies, thermodynamic properties and transition states [3]. The atmosphere is essentially a gaseous layer that surrounds Earth's lithosphere and hydrosphere and extends approximately 10,000 km from Earth's crust [4]. The atmosphere is composed of gas, solid and liquid particles in suspension, and its structure is nonhomogeneous [5, 6]. Because it is a nonhomogeneous system, the atmosphere can be divided into different main layers called the troposphere, stratosphere, mesosphere, thermosphere and an extensive layer transitioning to outer space called the exosphere. The troposphere, in which most living organisms exist, also contains virtually all atmospheric water and represents 90% of the total atmospheric mass [7]. This region can be divided into two parts: the planetary boundary layer, a relatively static 1-km-thick layer close to Earth's surface, and the free troposphere, a much more turbulent layer that extends from the end of the latter to the edge of the troposphere. The chemical reaction studied in this work, $\text{OH} + \text{CO} \rightarrow \text{H} + \text{CO}_2$, occurs in the free troposphere. The reaction between the OH radical and CO is of great

importance to both the combustion of hydrocarbons because it releases energy and atmospheric chemistry because it supplies atomic hydrogen [8–10]. This reaction has been the subject of many experimental [11–14], molecular [15] and ab initio theoretical studies in which the potential energy hypersurface of the reaction has been explored to find alternative paths and transition states using different calculation bases [16–18]. Thus, this paper proposes to explore the reaction, using the ab initio MøllerPlesset perturbation theory to the 2nd order (MP2) and the coupled cluster method with single and double excitations (CCSD) with a flexible 6-311++G(d,p) basis set [19, 20].

2. Theory and Computational Details

The equilibrium geometry of a molecule is the spatial configuration of the nuclei at which the electron energy is minimized. In diatomic molecules, the geometry is determined only by the bond length, but in polyatomic molecules, all nuclear coordinates (bond lengths and angles) must be specified. To determine the geometry of a polyatomic molecule, the derivative of the electronic energy with respect to each of the nuclear coordinates (the energy gradient) is numerically calculated. The energy is minimized when all energy gradient components are approximately zero. The structural geometries were optimized using the MP2 [21] and CCSD methods with the 6-311++G(d,p) basis set and Gaussian 09W [22, 23] software for all calculations. Given the optimized geometries, the frequencies were calculated to confirm that the resulting structures corresponded to the minimum energy conformations. In addition, the thermodynamic properties of the studied structures were obtained via frequency calculations. The energies were derived from calculations at the MP2 geometric level with a flexible 6-311++G(d,p) basis set, which includes both polarization and diffusion functions. The PES (Potential Energy Surface) examination will be performed to determine one or more possible

transition states. This method was implemented by H. B. Schlegel et al. [24] and begins with optimizing the geometries. Once the starting structures have been optimized, a quadratic synchronous transit (QST3 or QST2) calculation is performed. The QST2 requires the specification of two molecules, a reactant and a product, on the input route. The QST3 requires the specification of three molecules, the reactant, product and an initial structure, for the transition state in that specific order. After either or both of the calculations have been performed, the resulting structure is obtained, and a frequency calculation is performed. This step is crucial because it determines the possibility of a transition state. We review the vibrational frequencies, to see an imaginary frequency exists; if it does, we continue our search. After verifying the imaginary frequency, the IRC (intrinsic reaction coordinate) [25, 26] calculations are performed in which the initial geometry, given by the transition state, must be specified along with the path to follow in one or both directions. The geometry of the structure in question is optimized at each point of the reaction coordinate.

3. RESULTS AND DISCUSSION

Geometries and Energies

The geometries of the reactants and products were optimized using the aforementioned methodologies, finding the most stable structures for the different species. Through this, the bond length (\AA), angles ($^\circ$), and dihedral angles ($^\circ$) were determined and are provided in Table 1. The geometrical parameters reported in this table do not differ significantly when using different theoretical methodologies. After obtaining the minimum energy structures of the reactants and products, the QST3 and QST2 calculations were performed in which the possible stationary or transient structures were established. These structures were subsequently characterized using their vibrational normal modes, establishing that the molecules correspond either to minimums or transition states. Then, geometric optimization calculations were

performed as reported in Table 1. After optimizing the geometries, a third minimum-energy structure was established corresponding to the HCO₂ molecule, which has a dihedral angle of 180.0° because it derives from the trans geometric isomer. The first HCO₂ transition state was then observed in which the bond length corresponding to the hydrogen-carbon bond was approximately 0.65 \AA greater than the same value in the stationary structure. The angle corresponding to O1-C-O2 for the TS was approximately 35° greater than the minimum-energy structure due to the stereoelectronic repulsion of the oxygen lone pairs. The energies of the studied species could be obtained through the geometric optimizations if they corresponded to the reactants, minima, transition structures or products as reported in Table 2, which indicates that the minimum-energy or intermediate reaction states have a lower energy than the transition states. After calculating the energy, the frequency calculations were performed, and in these steps, the thermodynamic parameters were obtained from the statistical mechanics of the studied species as shown in Table 3. The energies obtained through the MP2 method were reported and corrected using the ZPE (zero-point energy), which indicates the ground state energy and the corrections to the enthalpy and Gibbs free energy.

Vibrational Normal Modes

The vibrational normal modes of the studied molecules are reported in Table 4. Molecules containing N atoms require $3N$ coordinates to describe their movements, $3N$ translational movements and $3N-6$ vibrational degrees of freedom. Each vibrational degree of freedom has a vibrational normal mode with specific symmetry properties such as symmetric extension, asymmetric extension and bending. Each of the studied structures exhibits six vibrational normal modes in which intermediate structures, which do not have an imaginary frequency, differ from the transition structures that do have an imaginary frequency. The transition structures were characterized by their imaginary

frequency and by performing IRC-type calculations, which connect the transition state with the intermediate structures, reactants or products.

Reaction Coordinates

Having characterized each of the previously described structures, IRC calculations were performed, finding two possible pathways for the studied reaction. These pathways have common structures, as shown in Figure 1, and the separation of these two possible pathways occurs with the formation of cis and trans geometric isomers. In Figure 1, three energy minima states are shown, the trans (HOCO) minimum, the cis (HOCO) minimum and the (HCO₂) minimum, two of which have similar energies (the cis and trans HOCO geometric isomers) but differ in their dihedral angles of 0.0° and 180.0°, respectively, with an energy difference of approximately 2 kcal/mol. The Hammond postulate [27, 28, 29] affirms that the structure of a transition state resembles that of the stable species (reactant or product) with the closest free energy. If the energy difference between the initial state and the transition state is small, the transition state is similar to the reactants as is the case in exothermic reactions. However, a transition state that more closely resembles the products than the reactants is said to be late (a late transition state) as is the case in endothermic reactions. Figure 2 shows that the reaction is exothermic with energy equal to -34.5 kcal/mol indicating that the reaction releases energy. This is confirmed by the fact that the cis HO CO (TS) and cis H OCO (TS) states have a Gibbs free energy values of -118376.435 kcal/mol and -118378.945 kcal/mol, respectively, which are close to those of the reagents. The reagents have an energy value of -118383.965 kcal/mol, which is larger than the energy of the products (-118417.223 kcal/mol). For the trans (HOCO) and cis (HOCO) minimum states, an endothermic reaction occurs with an energy of 1.883 kcal/mol resulting from the fact that the HOCO (TS) state has an energy value of -118399.026 kcal/mol, which approaches the energy of the cis

(HOCO) minimum state. The cis (HOCO) minimum state has a value of -118406.556 kcal/mol, rather than the energy of the trans (HOCO) minimum state, which has a Gibbs free energy of -118408.438 kcal/mol. The coordinates of the trans isomer are depicted in Figure 3; the corresponding reaction energy is -118383.965 kcal/mol, for both the trans HO CO (TS) at -118380.828 kcal/mol and the trans H OCO (TS) at -118368.278 kcal/mol. This reaction energy suggests a similarity to the reagents; therefore, according to the Hammond postulate, the reaction is exothermic.

The activation energy is the energy that a system requires to initiate a given process and is often used to describe the minimum energy required to produce a chemical reaction; that is, a reaction between two molecules occurs if they collide with the correct orientation and have a minimum amount of energy. Therefore, Figure 4 shows both the activation energy and the E for the studied reaction. A positive activation energy is observed for the trans HO CO transition state indicating that 3.138 kcal/mol is needed for this first reaction step to occur. An energy of 25.73 kcal/mol is released to reach the trans (HOCO) minimum state. Subsequently, an energy of 40.161 kcal/mol is absorbed to reach the trans (H OCO) transition state followed by an energy release of -18.83 kcal/mol to reach the H CO₂ transition state. Then, -1.255 kcal/mol of energy is released to reach the (HCO₂) minimum state. Finally, -28.87 kcal/mol of energy is released to yield the products. The cis reaction coordinates are shown in Figure 5 in which one can observe that the activation energy from the reagents to the first cis HO CO TS, thus the energy needed to perform this step, is 6.79 kcal/mol. Then, -25.73 kcal/mol will be produced to reach the trans (HOCO) minimum state. This state absorbs 10.04 kcal/mol of energy to reach the next HOCO (TS) transition state, which releases -8.16 kcal/mol, arriving at the cis (HOCO) minimum state. This state absorbs 28.24 kcal/mol to reach the cis H OCO TS state. Finally, -38.278 kcal/mol is released to arrive at the products.

Table 1
Geometric parameters (r and degrees (\angle)) of the studied molecules calculated with the MP2, B3LYP and HF models and the 6-311G basis set**

Parameter	MP2	B3LYP	HF
OH			
r (O-H)	1.000	1.000	1.000
CO			
r (C-O)	1.139	1.139	1.139
CO ₂			
r (C-O)	1.202	1.185	1.159
\angle (O-C-O)	180.00	180.00	180.00
cis (HOCO) minimum			
r (H-O ₁)	0.971	0.973	0.974
r (C-O ₁)	1.333	1.335	1.335
r (C-O ₂)	1.187	1.187	1.188
\angle (H-O ₁ -C)	106.88	107.51	107.51
\angle (O ₁ -C-O ₂)	130.37	130.18	130.18
\angle D (H-O ₁ -C-O ₂)	0.00	0.00	0.00
trans (HOCO) minimum			
r (H-O ₁)	0.964	0.964	0.964
r (C-O ₁)	1.349	1.349	1.349
r (C-O ₂)	1.183	1.183	1.183
\angle (H-O ₁ -C)	107.07	107.07	107.07
\angle (O ₁ -C-O ₂)	126.95	126.95	126.95
\angle D (H-O ₁ -C-O ₂)	180.00	180.00	180.00
(HOCO ₂) minimum			
r (H-C)	1.093	1.093	1.093
r (C-O ₁)	1.257	1.257	1.257
r (C-O ₂)	1.257	1.257	1.257
\angle (H-C-O ₁)	123.66	123.66	123.66
\angle (H-C-O ₂)	123.65	123.65	123.65
\angle (O ₁ -C-O ₂)	112.69	112.69	112.69
\angle D (H-O ₁ -C-O ₂)	180.00	180.00	180.00
H CO ₂ (TS)			
r (H-C)	1.177	1.164	1.093

Table 1 { Continued from the previous page

Parameter	MP2	B3LYP	HF
r (C-O ₁)	1.223	1.228	1.320
r (C-O ₂)	1.223	1.216	1.171
< (H-C-O ₁)	106.45	105.37	108.93
< (H-C-O ₂)	106.53	109.95	126.26
< (O ₁ -C-O ₂)	147.02	144.68	124.81
<D (H-O ₁ -C-O ₂)	180.00	180.00	180.00
cis H OCO (TS)			
r (H-O ₁)	0.971	0.977	0.950
r (C-O ₁)	1.333	1.326	1.307
r (C-O ₂)	1.188	1.183	1.159
< (H-O ₁ -C)	106.93	109.09	109.91
< (O ₁ -C-O ₂)	130.39	130.41	130.66
<D (H-O ₁ -C-O ₂)	0.00	0.00	0.00
HOCO (TS)			
r (H-O ₁)	0.967	0.967	0.969
r (C-O ₁)	1.369	1.370	1.365
r (C-O ₂)	1.182	1.182	1.176
< (H-O ₁ -C)	107.93	107.93	109.34
< (O ₁ -C-O ₂)	129.34	129.34	129.28
<D (H-O ₁ -C-O ₂)	86.80	86.80	86.92
cis HO CO (TS)			
r (H-O ₁)	0.972	0.978	0.950
r (C-O ₁)	1.333	1.323	1.308
r (C-O ₂)	1.188	1.183	1.159
< (H-O ₁ -C)	106.93	109.11	109.92
< (O ₁ -C-O ₂)	130.39	130.42	130.69
<D (H-O ₁ -C-O ₂)	0.00	0.01	0.00
trans HO CO (TS)			
r (H-O ₁)	1.923	1.910	1.968
r (C-O ₁)	1.223	1.226	1.321
r (C-O ₂)	1.223	1.226	1.321
< (H-O ₁ -C)	35.94	35.87	31.68
< (O ₁ -C-O ₂)	147.03	144.74	124.80
<D (H-O ₁ -C-O ₂)	180.00	180.00	180.00

Table 1 { Continued from the previous page

Parameter	MP2	B3LYP	HF
trans H O CO (TS)			
r (H-O ₁)	1.247	1.247	1.247
r (C-O ₁)	1.304	1.304	1.304
r (C-O ₂)	1.180	1.180	1.180
< (H-O ₁ -C)	62.00	62.00	62.00
< (O ₁ -C-O ₂)	143.28	143.28	143.28
<D (H-O ₁ -C-O ₂)	180.00	180.00	180.00

Table 2
Energies (in hartrees) of the studied molecules at different calculation levels

Parameter	HF-6-311G**	B3LYP-6-311G**	MP2-6-311G**
OH	-75.413	-75.762	-75.413
CO	-112.768	-113.349	-112.751
CO ₂	-187.566	-188.557	-187.559
cis (HOCO) minimum	-188.184	-189.152	-188.690
trans (HOCO) minimum	-188.185	-189.154	-188.693
(HOCO ₂) minimum	-188.145	-189.135	-188.663
H CO ₂ (TS)	-188.127	-189.115	-188.656
cis H OCO (TS)	-188.117	-189.113	-188.639
trans H OCO (TS)	-188.100	-189.095	-188.623
HOCO (TS)	-188.150	-189.138	-188.676
cis HO CO (TS)	-188.146	-189.106	-188.634
trans HO CO (TS)	-188.164	-189.108	-188.643

Table 3
Thermodynamical parameters (in hartrees) of the studied molecules at the MP26-311G level**

Parameter	E ₀	H _{corr}	G _{corr}	E ₀ + ZPE	E ₀ + H _{corr}	E ₀ + G _{corr}	ZPE
OH	-75.41	0.011	-0.009	-75.41	-75.40	-75.42	0.011
CO	-112.75	0.008	-0.014	-112.75	-112.74	-112.77	0.008
CO ₂	-187.56	0.014	-0.011	-187.55	-187.55	-187.57	0.015
cis (HOCO) minimum	-188.69	0.025	-0.003	-188.67	-188.67	-188.69	0.021
trans (HOCO) minimum	-188.69	0.025	-0.003	-188.67	-188.67	-188.69	0.021
(HOCO ₂) minimum	-188.69	0.027	-0.002	-188.64	-188.64	-188.67	0.023
H CO ₂ (TS)	-188.66	0.022	-0.007	-188.64	-188.63	-188.66	0.018
cis H OCO (TS)	-188.64	0.019	-0.010	-188.62	-188.62	-188.65	0.015
trans H OCO (TS)	-188.62	0.019	-0.009	-188.61	-188.60	-188.63	0.015
HOCO (TS)	-188.68	0.024	-0.005	-188.66	-188.65	-188.68	0.020
cis HO CO (TS)	-188.63	0.021	-0.011	-188.62	-188.61	-188.65	0.016
trans HO CO (TS)	-188.64	0.021	-0.009	-188.63	-188.62	-188.65	0.016

Table 4
Vibrational normal modes of the studied molecules

Method	Frequencies (cm ⁻¹)
trans HO CO (TS)	
HF/6-311G**	341.92i/448.23/598.70/1054.85/2148.57/3800.41
B3LYP/6-311G**	250.36i/133.70/292.47/658.34/2125.02/3769.75
MP2/6-311G**	142.69i/190.61/290.43/676.79/2155.28/3806.66
cis HO CO (TS)	
HF/6-311G**	319.22i/118.86/135.32/788.92/2150.93/3759.83
B3LYP/6-311G**	510.56i/173.04/333.55/991.46/2096.42/3718.27
MP2/6-311G**	319.22i/118.86/135.32/788.92/2150.93/3759.46
trans HOCO minimum	
HF/6-311G**	717.55/741.74/1101.92/1447.17/1901.13/3869.28
B3LYP/6-311G**	529.66/620.03/1070.62/1245.24/1878.62/3828.08
MP2/6-311G**	564.98/622.35/1107.74/1266.58/196.44/3865.90
HOCO (TS)	
HF/6-311G**	532.11i/753.24/1289.18/1636.78/2134.68/3823.54
B3LYP/6-311G**	618.74i/649.81/959.08/1090.78/1855.07/3784.31
MP2/6-311G**	620.43i/656.14/998.52/1107.33/1992.03/3831.95
cis HOCO minimum	
HF/6-311G**	705.11/815.82/1160.20/1478.51/1867.15/3723.89
B3LYP/6-311G**	583.55/602.19/1048.34/1303.43/1840.99/3644.66
MP2/6-311G**	617.76/619.28/1106.20/1323.56/1887.20/3705.65
trans H OCO (TS)	
HF/6-311G**	2369.66i/711.39/744.87/1111.56/1832.57/2241.58
B3LYP/6-311G**	1832.97i/535.66/680.51/1124.64/1829.44/2138.94
MP2/6-311G**	1932.39i/588.99/720.63/1214.47/1882.95/2262.92
HCO ₂ minimum	
HF/6-311G**	690.69/1246.63/1354.81/1510.68/1852.03/3183.13
B3LYP/6-311G**	658.25/1017.56/1023.70/1279.41/1476.91/3091.48
MP2/6-311G**	671.10/1165.05/1300.66/1506.40/2254.22/3160.78

Table 4 { Continued from the previous page

Method	Frequencies (cm ⁻¹)
H CO ₂ (TS)	
HF/6-311G**	1579.14i/811.10/853.99/1116.00/1443.72/2069.86
B3LYP/6-311G**	977.78i/670.22/711.80/1046.50/1432.64/2151.64
MP2/6-311G**	702.64i/479.84/693.21/983.83/1391.78/2182.32
cis H OCO (TS)	
HF/6-311G**	2951.97i/670.16/797.75/1124.05/1299.61/2117.80
B3LYP/6-311G**	1654.27i/618.57/681.38/1045.81/1325.93/2165.00
MP2/6-311G**	1525.80i/479.84/693.21/983.83/1391.78/2182.32

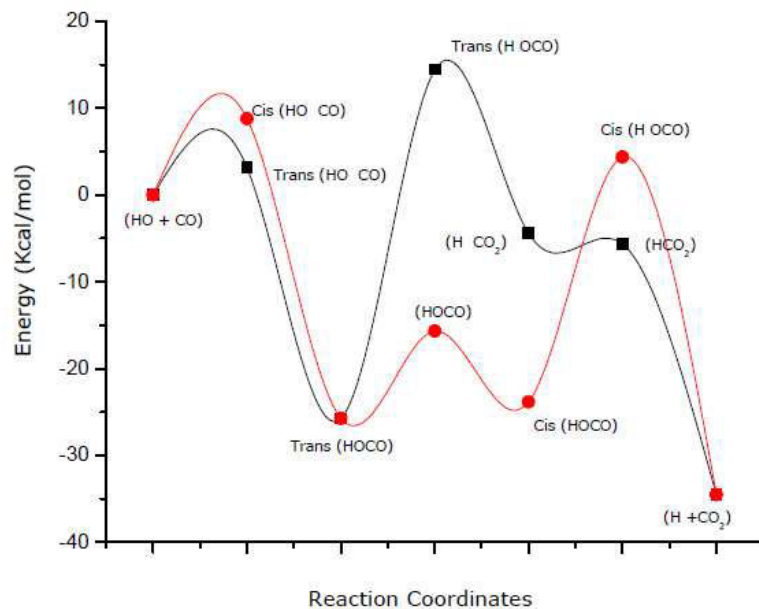


Figure 1
Potential energy surface for the studied reaction

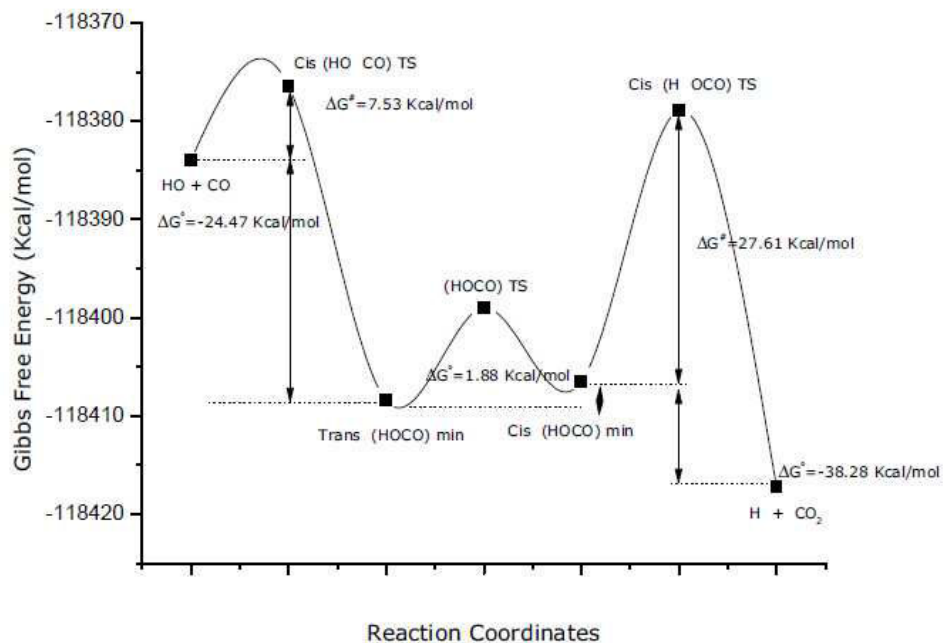


Figure 2
Gibbs free energy surface for the cis isomer

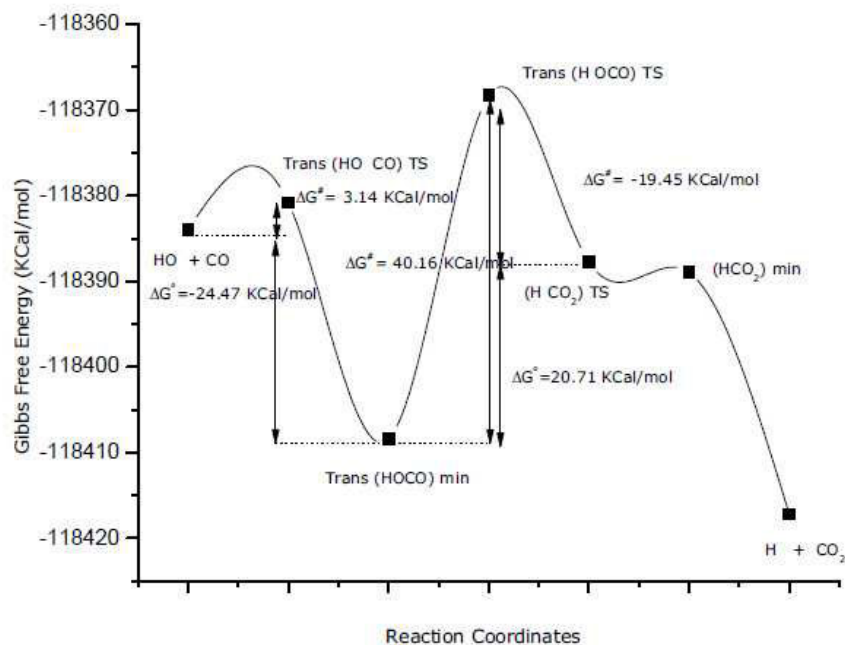


Figure 3
Gibbs free energy surface for the trans isomer

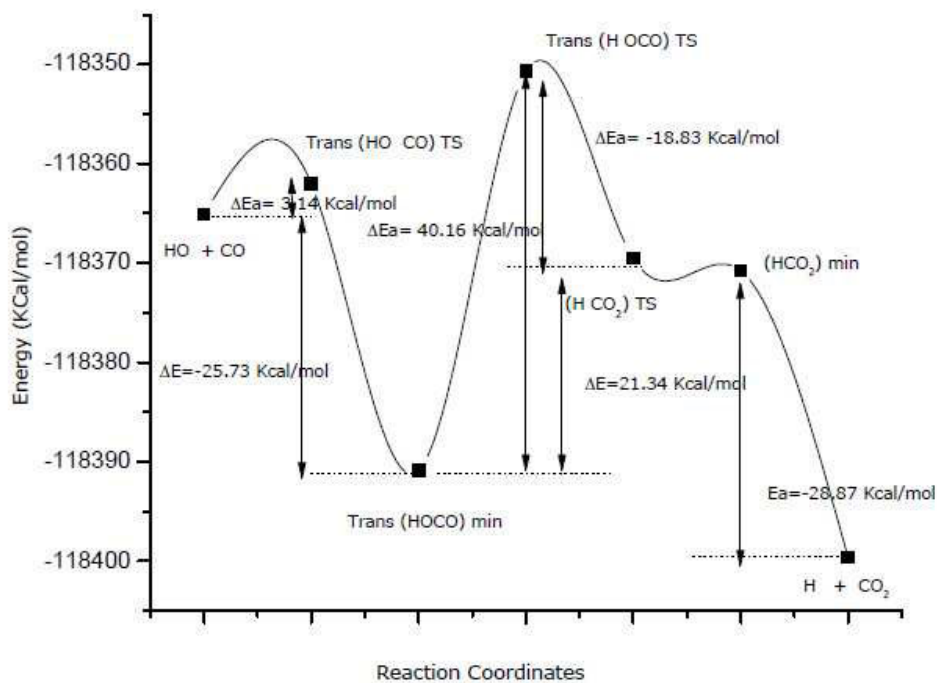


Figure 4
Activation energies for each of the structures through the trans isomer

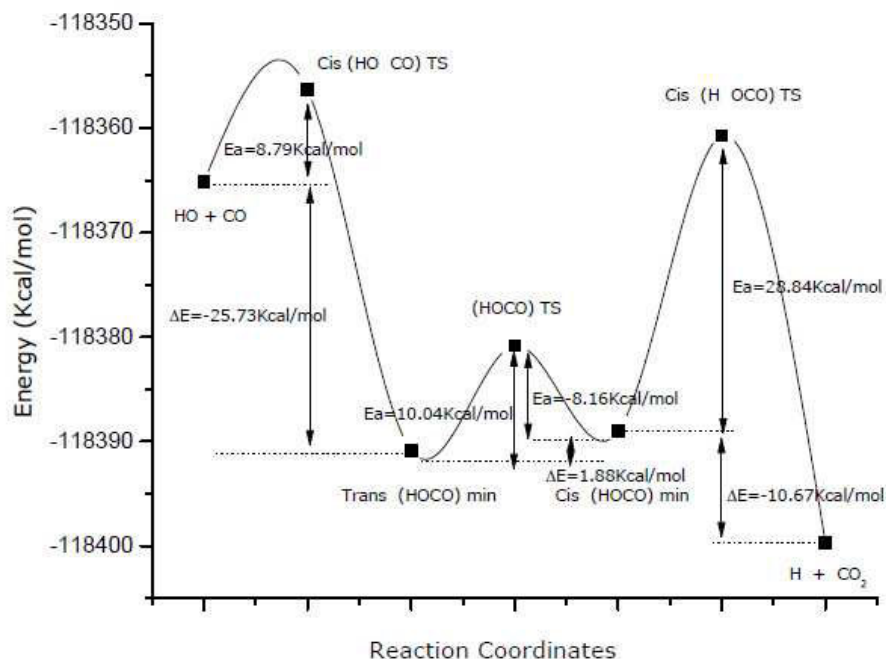


Figure 5
Activation energies for each of the structures through the cis isomer

4. CONCLUSIONS

- The use of HF, MP2, and B3LYP methodologies provided relevant information on the considered reaction.
- The hydroxyl radical reacts with carbon monoxide to form cis- and trans-type geometric isomers for the HOCO structure.
- Six transition states were found and characterized using their imaginary frequencies and their connections to stationary points.
- Three minimum or intermediate reaction states were obtained with lower energies than the reactants and greater energies than the products, indicating that these minimum states are more stable in the atmosphere than the reactants and less stable than the products.
- The reaction under consideration has two possible reaction pathways, one via the cis geometrical isomer and the other through the trans geometrical isomer.

- The overall reaction is exothermic with $\Delta H = -34.51$ kcal/mol.
- According to the Hammond postulate, the transition states participate- in the considered reaction are similar in energy to the reactants; therefore, the reaction is exothermic.

ACKNOWLEDGEMENTS

This work was supported by operating grants N°01/2011 from the Universidad Católica de la Santísima Concepción (Chile). Also, this work has been partially supported by CIMAV, SC and Consejo Nacional de Ciencia y Tecnología (CONACYT, Mexico). DGM is a researcher of CONACYT and CIMAV. The authors are imdebted to the late Ph.D Guillermo Contreras Koder for all his contributions to science.

REFERENCES

1. S. Sander, R. Friedl, D. Golden, M. Kurylo, G. Moortgat, H. Keller- Rudek, P. Wine, A. Ravishankara, C. Kolb, M. Molina, B. Finlayson- Pitts, R. Huie, V. Orkin, Chemical kinetics and photochemical data for use in atmospheric studies – Evaluation Number 15 (2006).
2. E. Wilkins, Air pollution and the London fog of December, Journal of the Royal Sanitary Institute 74 (1954) 14.
3. J. Wallace, P. Hobbs, Atmospheric Science: An Introductory Survey, 2nd Edition, Academic Press, Burlington, MA, 2006.
4. R. Wayne, Chemistry of Atmospheres, 3rd Edition, Oxford University Press, New York, 2000.
5. S. Chapman, A theory of upper-atmosphere ozone, Memories of the Royal Meteorologic Society 3 (1930) 103.
6. M. Molina, F. Rowland, Stratospheric sink for chlorofluoromethanes: Chlorine atom catalyzed destruction of ozone, Nature 249 (1974) 810– 812.
7. C. Wayne, R. Wayne, Photochemistry, Oxford Chemistry Primers, Oxford University Press, Oxford, UK, 1996.
8. D. Albritton, M. Allen, WG1 Report – Climate change: The scientific basis: Summary for policymakers (2001).
9. C. Bentley, Rapid sea-level rise soon from west antarctic ice-sheet collapse?, Science 275 (1997) 1077–1078.
10. D. Jacob, The oxidizing power of the atmosphere, in: T. Potter, B. Colman, J. Fishman (Eds.), Handbook of Weather, Climate and Water, McGraw-Hill, 2000.
11. G. Dawson, Atmospheric ammonia from undisturbed land, Journal of Geophysical Research 82 (1977) 3125.
12. T. Graedel, The kinetic photochemistry of the marine atmosphere, Journal of Geophysical Research 84 (1979) 273.
13. D. Jacob, M. Hoffmann, A dynamic model for the production of H^+ , NO_3^- , and SO_4^{2-} in urban fog, Journal of Geophysical Research 88 (1983) 6611–6621.
14. H. Kurasawa, R. Lesclaux, Rate constant for the reaction of NH_2 with ozone in relation to atmospheric processes, Chemical Physics Letters 72 (1980) 437–442.
15. V. Bulatov, A. Buloyan, S. Cheskis, M. Kozliner, O. Sarkisov, A. Trostin, On the reaction of the NH_2 radical with ozone, Chemical Physics Letters 74 (1980) 288–292.
16. H. Yu, J. Muckerman, T. Sears, A theoretical study of the potential energy surface for the reaction $OH + CO \leftarrow H + CO_2$, Chemical Physics Letters 349 (2001) 547–554.
17. D. Zhang, J. Zhang, Quantum calculations of reaction probabilities for $HO + CO \rightarrow H + CO_2$ and bound states of $hoco$, Journal of Chemical Physics 103 (1995) 6512–6519.
18. R. Zhu, E. Diau, M. Lin, A. Mebel, A computational study of the $OH(OD) + CO$ reactions: Effects of pressure, temperature, and quantum-mechanical tunneling on product formation, Journal of Physical Chemistry 105 (2001) 11249–11259.
19. W. Hehre, L. Radom, P. v. Schleyer, J. Pople, Ab Initio Molecular Orbital Theory, John Wiley & Sons, New York, 1986.
20. R. Parr, W. Yang, Density functional theory of the electronic structure of molecules, Annual Review of Physical Chemistry 46 (1995) 701–728.
21. C. Møller, M. Plesset, Note on an approximation treatment for many-electron systems, Physical Review 46 (1934) 618–622.
22. M. J. Frisch, G. W. Trucks, H. B. Schlegel, G. E. Scuseria, M. A. Robb, J. R. Cheeseman, G. Scalmani, V. Barone, B. Mennucci, G. A. Petersson, H. Nakatsuji, M. Caricato, X. Li, H. P. Hratchian, A. F. Izmaylov, J. Bloino, G. Zheng, J. L. Sonnenberg, M. Hada, M. Ehara, K. Toyota, R. Fukuda, J. Hasegawa, M. Ishida, T. Nakajima, Y.

- Honda, O. Kitao, H. Nakai, T. Vreven, J. A. Montgomery, Jr., J. E. Peralta, F. Ogliaro, M. Bearpark, J. J. Heyd, E. Brothers, K. N. Kudin, V. N. Staroverov, R. Kobayashi, J. Normand, K. Raghavachari, A. Rendell, J. C. Burant, S. S. Iyengar, J. Tomasi, M. Cossi, N. Rega, J. M. Millam, M. Klene, J. E. Knox, J. B. Cross, V. Bakken, C. Adamo, J. Jaramillo, R. Gomperts, R. E. Stratmann, O. Yazyev, A. J. Austin, R. Cammi, C. Pomelli, J. W. Ochterski, R. L. Martin, K. Morokuma, V. G. Zakrzewski, G. A. Voth, P. Salvador, J. J. Dannenberg, S. Dapprich, A. D. Daniels, J. B. Foresman, J. V. Ortiz, J. Cioslowski, D. J. Fox, Gaussian 09 Revision A.1, gaussian Inc. Wallingford CT 2009.
23. J. Foresman, A. Frisch, Exploring Chemistry with Electronic Structure Methods, Gaussian, Inc, Pittsburgh, 1996.
24. C. Peng, H. Schlegel, Combining synchronous transit and quasi-newton methods for finding transition states, Israel Journal of Chemistry 33 (1994) 440.
25. C. González, H. Schlegel, An improved algorithm for reaction path following, Journal of Chemical Physics 90 (1990) 2154.
26. C. González, H. Schlegel, Reaction path following in mass-weighted internal coordinates, Journal of Physical Chemistry 94 (1994) 5523.
27. G. Hammond, A correlation of reaction rates, Journal of the American Chemical Society 77 (1955) 334–338.
28. R. Marcus, Chemical and electrochemical electron-transfer theory, Annual Review of Physical Chemistry 15 (1964) 155–196.
29. Swarnla, Panchl, et. Al, Int J Pharm Bio Sci 2012 July ; 3(3): B 202- 208